Polarization Inhomogeneity Effects in Microwave Fourier Transform Spectroscopy

W. Stahl and H. Dreizler

Abteilung Chemische Physik im Institut für Physikalische Chemie der Universität Kiel

In this paper two new experiments in microwave Fourier transform spectroscopy are presented: The first one gives an experimental evidence of the polarization inhomogeneity that occurs when a microwave pulse passes through a waveguide which is filled with a molecular sample at low pressure. In the second experiment a similar technique is applied to a double resonance experiment in order to show polarization inhomogeneity effects caused by the pump signal. The theoretical treatment is given in terms of the density matrix formalism.

Introduction

Some years ago we performed a microwave-microwave double resonance experiment using microwave Fourier transform technique (MWFTDR) [1]. Carbonylsulfide, OCS, was used as a sample. The level scheme is given in Fig. 1 of [1]. In the frequency domain it was observed that the signals produced by the double resonance effect are much broader than those produced by conventional microwave Fourier transform (MWFT) spectroscopy as shown in Fig. 3 of [1].

This fact can also be observed in the time domain. The signal of the conventional experiment is a decay caused by relaxation while, in comparison, that in presence of pump radiation is different in form and much shorter. Both cases are illustrated in Fig. 1a and b. It may be suspected that the inhomogeneity of the polarization in the waveguide gives an important contribution to this effect. This would mean, that the polarization does not decay primarily by an irreversible process like T_2-relaxation. As the conventional MWFT-spectrometers [2–6]* are constructed in a way that only the fundamental mode exists in the waveguide system, it is more precisely the projection of the polarization to the fundamental mode which decreases so rapidly. For MWFTDR-spectrometers with higher pump frequencies [1] several modes of the pump radiation exist necessarily in the sample cell.

---

* It is useful to use the fundamental mode in a MWFT-spectrometer only as reflections of the polarizing MW-pulse increase when higher modes are possible.

Reprint requests to Prof. Dr. H. Dreizler, Institut für Physikalische Chemie, Olshausenstr. 40 – 60, D-2300 Kiel.

To proof this picture we designed two new pulse experiments with the FT-technique. The first and simpler one gives the idea. The second is an extension to a double resonance experiment to explain the initial observation.

The result will be, that the large line width or rapid decay of the transient signal in a double resonance experiment is mainly due to the field inhomogeneity of the pump radiation.

The experiments will be described theoretically by a Bloch equation formalism, which was adjusted to the considered cases.
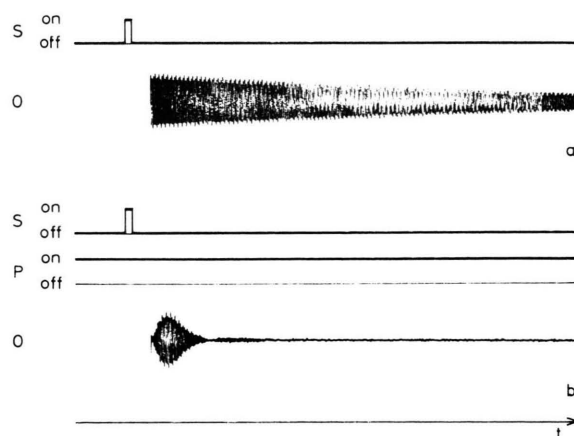

Fig. 1. a) Polarizing pulse and measured transient emission signal (O) in conventional MWFT-spectroscopy. The position of the polarizing pulse (S) is drawn schematically. The measurement is typically started after a delay of 200 to 1000 ns. b) Polarizing pulse (S) and measured transient emission signal (O) in the presence of resonant continuous wave pump radiation (P).

Experiment with Phase Inversion within the Polarizing Pulse in a Conventional MWFT-Experiment

In a conventional MWFT-experiment the molecular ensemble is polarized by a MW-pulse with a length of typically 50 to 1000 ns. The frequency of the carrier pulse is usually near the transition frequency, which is intended to be measured. Henceforth we will consider only the resonant case. The pulse power may be varied from some mW to the limit of the travelling wave tube amplifier (TWTA), say 20 W. Pulse length and power are adjusted to achieve $\pi/2$-conditions [7] as good as possible. The creation of polarization is connected with transient absorption and can be observed by a bridge type spectrometer [8]. Such an observation is not possible with a MWFT-spectrometer, as the strong polarizing pulse prevents the observation. As it is further difficult to suppress perturbations caused by the polarizing pulse the observation of the molecular signal is initiated with a delay between 200 and 1000 ns after the terminal edge of the pulse. The maximum amplitude of the transient signal observed after a delay can be taken as a measure of the created polarization. If the intensity I, the squared amplitude, is plotted against the pulse length τ at constant pulse power an oscillatory dependence is observed as indicated in Figure 2a. Qualitatively this is predicted by the theory assuming a plane wave [9]. The exponential decrease of the sine-function is determined by relaxation. Taking for OCS a pressure of 1 mTorr and $T_2 = 27\,\mu s$ one gets a slope of $\Delta I/\Delta \tau = 0.004/(100\,\text{ns})$ for the change ΔI of the maxima at $\pi/2$- and $3\pi/2$-pulses which are typically at $\tau_{\pi/2} = 50$ ns and $\tau_{3\pi/2} = 150$ ns. This minor decrease in I can not be seen in Figure 2a. But Fig. 2a resulting from simplified theoretical considerations is misleading as it is more and more difficult to observe experimentally $(2n+1)\pi/2$- or $n\pi$-pulses with higher $n > 2$. A more detailed consideration taking the field inhomogeneity across the waveguide into account* is necessary. With neglection of relaxation the square of a Bessel function (see below) describes the oscillatory behaviour of I as given in Figure 2b. It was roughly drawn according to oscilloscope measure-

---

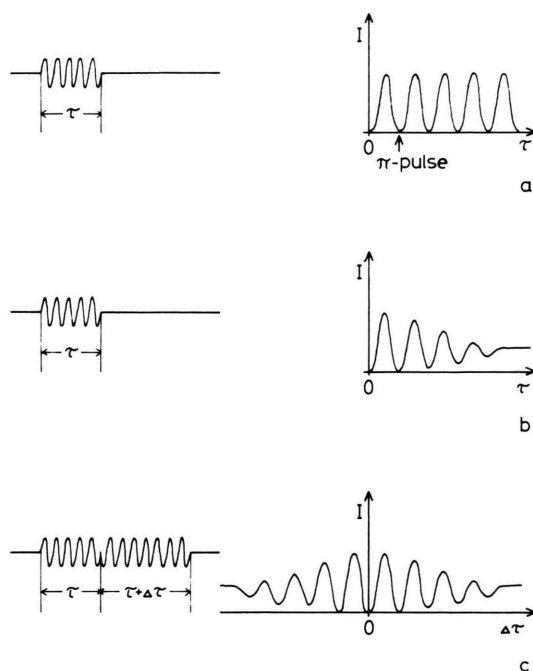* The inhomogeneity along the waveguide will be neglected.

Fig. 2. a) Dependence of the square I of the maximum amplitude of a transient decay assuming a plane polarizing wave from the pulse length τ with the field strength of the polarizing pulse fixed. Drawn according to theory [9]. The effect of relaxation cannot be seen within the scale of the figure. b) Dependence of the square I of the maximum amplitude of a transient decay in a waveguide from pulse length τ with field strength of the polarizing pulse fixed roughly drawn from oscilloscope measurements. c) Dependence of the square I of the maximum amplitude of a transient decay from the unbalance $\Delta \tau$ in length of two pulses with opposite phase. The effect of the first pulse is cancelled by part of the second of length $\tau + \Delta \tau$. Roughly drawn from oscilloscope measurements.

ments. The slope $\Delta I/\Delta \tau$ for the first two maxima, which correspond to $\pi/2$- and $3\pi/2$-pulses, is $\Delta I/\Delta \tau = 0.46/100$ ns when a difference of $\Delta \tau = 100$ ns is assumed.

For illustration we give in Fig. 3 the calculated distributions of polarization across the waveguide as it develops with pulse length τ. Only the projection of the polarization to the ground mode gives rise to the observable transient emission.

A simple way to show the influence of inhomogeneity of the polarizing field is to extend the polarizing pulse immediately after its end by a second one of equal frequency and power, of adjustable length $\tau + \Delta \tau$ but shifted in phase by π. A large amplitude of I can be regained. When the
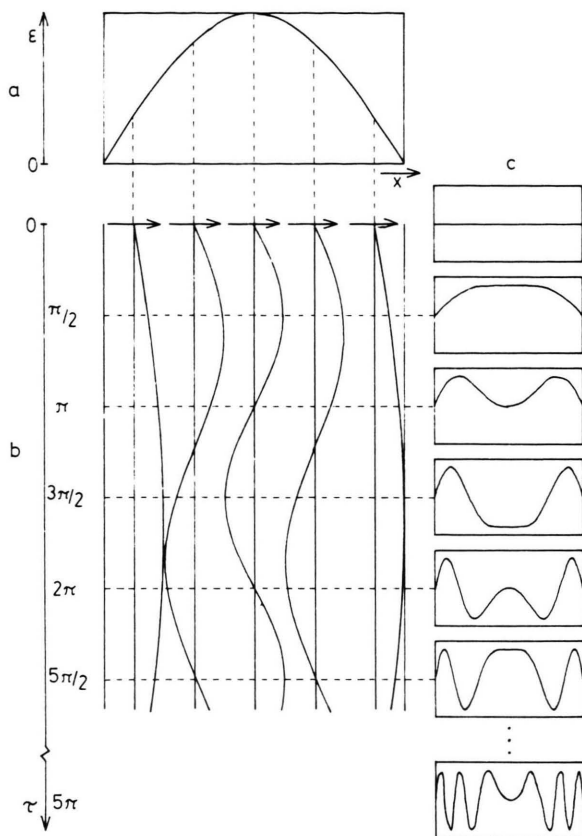
Fig. 3. a) Field distribution of the H_{10} fundamental mode in a waveguide of rectangular cross section. b) Dependence of polarization with pulse length τ at different positions x along the broad side of the waveguide. The position z along the waveguide length is fixed. c) Distribution of polarization − in the cross section at different pulse lengths τ.

pulse length of the second pulse is adjusted to $\tau (\Delta \tau = 0)$, $I = 0$ results. If $\Delta \tau > 0$ a dependence $I (\Delta \tau)$ results as given in Figure 2c. Also Fig. 2c is drawn according to oscilloscope measurements. It is equal to that of Fig. 2b with $\tau > 0$ replaced by $\Delta \tau$. With $\Delta \tau < 0$ the mirror image of $\Delta \tau > 0$ occurs. The phase change by π operates as if the time would be reversed.

If the irreversible relaxation would have been dominant it would be impossible to regain large amplitudes at the pulse length 2τ comparable to those near $\tau = 0$. Only the small difference between the intensities of the decay and its "echo" is the effect of relaxation. Thus the main reason for the damping of the oscillations is the field inhomogeneity.

Two Level Bloch Equations for Phase Inverted Pulses

The Bloch equations result from the time development of a two level density matrix described by [10]:

$$i \hbar \dot{\varrho} = [\hat{H}, \varrho], \tag{1}$$

where ϱ is the density matrix, $\hat{H}$ the Hamiltonian including molecule-electromagnetic field interaction. Assuming the dipole matrix elements $\mu_{aa} = 0$ and $\mu_{bb} = 0$, a and b designate the two levels, the matrix elements are:

$$H_{aa} = E_a,$$
$$H_{bb} = E_b,$$
$$H_{ab} = H_{ba} = -2\mu_{ab} \cdot \varepsilon \cdot \cos(\omega t + \varphi); \tag{2 a–c}$$

2ε is the amplitude of the microwave field, $\omega = 2\pi v$ its angular frequency, φ its phase, μ_{ab} a dipole matrix element, t the time. The equations are formulated for a certain volume element at a place z along the waveguide. The dependence from z is not considered. Working out the commutator of (1) one gets four differential equations for the density matrix elements.

$$\dot{\varrho}_{aa} = i \varkappa \varepsilon (\varrho_{ba} - \varrho_{ab}) \cdot \cos(\omega t + \varphi),$$
$$\dot{\varrho}_{bb} = -i \varkappa \varepsilon (\varrho_{ba} - \varrho_{ab}) \cdot \cos(\omega t + \varphi),$$
$$\dot{\varrho}_{ab} = i \omega_0 \varrho_{ab} + i \varkappa \varepsilon (\varrho_{bb} - \varrho_{aa}) \cdot \cos(\omega t + \varphi),$$
$$\dot{\varrho}_{ba} = -i \omega_0 \varrho_{ba} - i \varkappa \varepsilon (\varrho_{bb} - \varrho_{aa}) \cdot \cos(\omega t + \varphi),$$
$$\varrho_{ba} = \varrho_{ab}^*, \quad \varkappa = 2\mu_{ab}/\hbar, \quad \omega_0 = (E_b - E_a)/\hbar. \tag{3 a–d}$$

Transforming to a rotating frame by

$$\varrho_{aa} = \tilde{\varrho}_{aa},$$
$$\varrho_{bb} = \tilde{\varrho}_{bb},$$
$$\varrho_{ab} = \tilde{\varrho}_{ab} \cdot \exp(i \omega t),$$
$$\varrho_{ba} = \tilde{\varrho}_{ba} \cdot \exp(-i \omega t), \tag{4 a–d}$$

and using the rotating wave approximation and setting

$$\tilde{\varrho}_{aa} + \tilde{\varrho}_{bb} = s,$$
$$\tilde{\varrho}_{ab} + \tilde{\varrho}_{ba} = u,$$
$$i (\tilde{\varrho}_{ba} - \tilde{\varrho}_{ab}) = v,$$
$$\tilde{\varrho}_{aa} - \tilde{\varrho}_{bb} = w \tag{5 a–d}$$

one gets

$$\dot{s} = 0,$$

$$\dot{u} = -(\Delta\omega)v + \varkappa\varepsilon w \cdot \sin\varphi,$$

$$\dot{v} = (\Delta\omega)u - \varkappa\varepsilon w \cdot \cos\varphi,$$

$$\dot{w} = \varkappa\varepsilon(v \cdot \cos\varphi - u \cdot \sin\varphi) \qquad (6\,a-d)$$

with

$$\Delta\omega = \omega_0 - \omega.$$

It should be pointed out, that relaxation is not included in (6). The equations are formulated for a plane electromagnetic wave. No mode structure is incorporated. For $\varphi = 0$ the equations (6) are the usual Bloch equations without relaxation.

It is interesting to formulate solutions of (6). Assuming a pulse of length $\tau = (t_1 - t_0)$ and $\varphi = 0$ and starting with thermal equilibrium and resonance: $\Delta\omega = 0$ yields

$$s(t_1 - t_0) = u(t_1 - t_0) = 0,$$

$$\begin{aligned} v(t_1 - t_0) &= -w(t_0) \cdot \sin[\varkappa\varepsilon(t_1 - t_0)] \\ &= -w(t_0) \cdot \sin(\varkappa\varepsilon\tau), \end{aligned}$$

$$\begin{aligned} w(t_1 - t_0) &= w(t_0) \cdot \cos[\varkappa\varepsilon(t_1 - t_0)] \\ &= w(t_0) \cdot \cos(\varkappa\varepsilon\tau). \end{aligned} \qquad (7\,a-c)$$

For an immediately following pulse of length $t_2 - t_1$ and phase $\varphi = \pi$ and with $(7\,a-c)$ at time t_1 as initial condition the final solutions are:

$$s(t_2 - t_1) = u(t_2 - t_1) = 0,$$

$$\begin{aligned} v(t_2 - t_1) &= w(t_0) \cdot \sin\{\varkappa\varepsilon[(t_1 - t_0) - (t_2 - t_1)]\} \\ &= -w(t_0) \cdot \sin[\varkappa\varepsilon(\Delta\tau)], \end{aligned}$$

$$\begin{aligned} w(t_2 - t_1) &= w(t_0) \cdot \cos\{\varkappa\varepsilon[(t_1 - t_0) - (t_2 - t_1)]\} \\ &= w(t_0) \cdot \cos[\varkappa\varepsilon(\Delta\tau)]. \end{aligned} \qquad (8\,a-c)$$

If the lengths $t_1 - t_0$ and $t_2 - t_1$ are equal the initial conditions at time t_0 are reproduced. The phase inverted second pulse cancels the effect of the first one. If the lengths are out of balance $\Delta\tau = (t_2 - t_1) - (t_1 - t_0)$ a solution in $\Delta\tau$ as time instead $t_1 - t_0$ analog to $(7\,a-d)$ results.

Mode inhomogeneity and relaxation is still not included, but (8) describes the essential features of the experiment. The phase inverted pulse has consequences like a negative time.

Influence of Mode Inhomogeneity

The Eqs. (7) and (8) were derived as resonant solutions of two level Bloch equations (6) with $\varphi = 0$
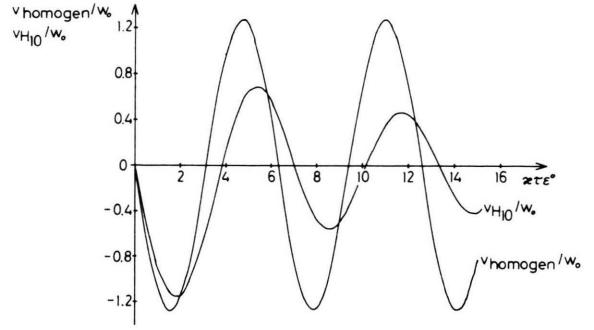

Fig. 4. Comparison of solutions $(7\,b)$ v_{homogen}/w_0 $(w_0 = w(t_0))$ with assumption of plane wave and (9) $v_{H_{10}}/w_0$ with assumption of H_{10} waveguide mode.

and $\varphi = \pi$. As a volume element along the waveguide was considered the variable in (6) is only time. For simplicity a plane wave was assumed. The mode inhomogeneity may be introduced for the ground mode H_{10} (TE$_{10}$) of the waveguide by setting $\varepsilon = \varepsilon(x) = \varepsilon^0 \sin(x\pi/a)$, where a is the width of the waveguide, x the coordinate in this direction (see Figure 3).

By projecting the polarization

$$v(t - t_0) = \sin[\varkappa(t - t_0)\varepsilon^0] \cdot \sin(x\pi/a)$$

which contains the dependence of $\varepsilon = \varepsilon(x)$ of the H_{10} fundamental mode one gets [11]:

$$v_{H_{10}}(t - t_0) = -2w(t_0) J_1(\varkappa\varepsilon^0\tau) \qquad (9)$$

with the first order Bessel function J_1. A comparison with $(7\,b)$ is given in Figure 4. The degree of inhomogeneity is given by the magnitude of ε^0 as the field ε in the waveguide is zero at $x = 0$ and $x = a$. Increasing ε^0 contracts the curve representing (9) giving a steeper slope of its envelope. Qualitatively Fig. 2b results by squaring (9).

The difference in the asymptotic behaviour results from the fact that (9) gives a solution for infinite relaxation time. As the relaxation time is finite, (9) is not a suitable asymptotic solution. The incorporation of relaxation in addition to mode inhomogeneity complicates the treatment of transient absorption.

Further the movement of the molecules and wall collisions should be included *. We do not try to give a solution here.

---

* For a treatment of transient emission including these effects see [12].

In an analog procedure the solutions (8) of the Bloch equations (6) with $\varphi = \pi$ can be modified. The principle behaviour of the time dependence is not changed.

We think that the last two sections give an explanation of the first experiment.

Double Resonance Experiment with Phase Inversion of the Pump Radiation

If in a MWFTDR experiment the pump radiation is applied continuously the observed transient signal has the shape of Figure 1 b. The double resonance effect, the splitting of the transition, is observable in a wide range of pump powers from some mWatts to some Watts. For higher pump powers the transient signal decays faster or the double resonance lines are broader. For simplicity we consider resonant pump radiation. If the pump radiation is off resonant by some MHz, the double resonance effect vanishes and the narrow single resonance signal of the conventional experiment remains. It will be shown that the rapid decay is a consequence of the pump field strength and inhomogeneity.
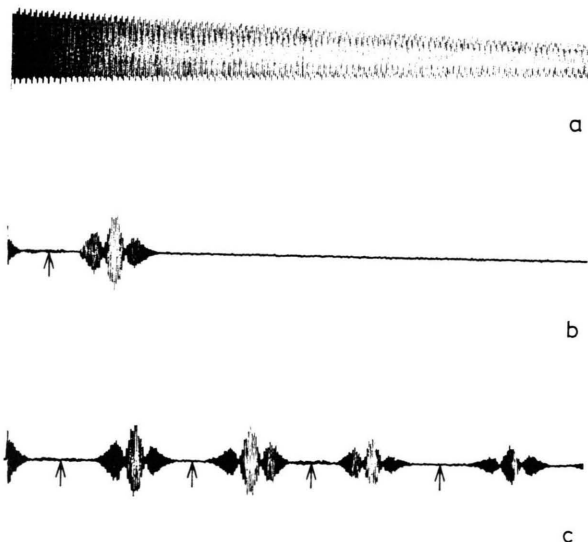

a

b

c

Fig. 5. a) Transient emission signal in conventional MWFT-spectroscopy for comparison. b) "Echo" signal with a continuous pump power phase inverted at time τ marked by an arrow. The "echo" signal reaches its maximum intensity at 2τ. c) Chain of echo signals produced by multiple phase inversion of the continuous pump power. Inversion points are indicated by arrows. Fig. 5a, b and c are recorded at constant pressure and temperature.

If the pump experiment is modified by phase shifting the pump radiation by π after the transient signal has vanished the observation is drastically changed. A transient signal reappears and decays again as illustrated in Figure 5 b. When the phase is shifted again by π the effect can be repeated several times as shown in Figure 5 c. Each phase shift produces a new observable "echo" signal. The relative magnitude of the recovered signals decrease in the same time as a molecular transient signal decays in a conventional MWFT experiment. Thus the envelope of Fig. 5 c is equal to that of Fig. 5 a showing relaxation. As the signal can be recovered the rapid decay of a single signal cannot be due to an irreversible process like relaxation.

Three Level Bloch Equations Including Phase Inversion of the Pump

The Bloch equations for a three level system as given in Fig. 1 of [1] are based on (1) with ϱ a density matrix for three levels a, b, and c. We assume: 1) the phase of the signal microwave is constant, 2) the phase φ of the pump microwave is variable, 3) relaxation is neglected and 4) the dipole matrix elements are:

$$\mu_{aa} = \mu_{bb} = \mu_{cc} = \mu_{ac} = 0,$$
$$\mu_{ab} \neq 0, \quad \mu_{bc} \neq 0. \tag{10}$$

The assumption 4) applies to OCS.

The matrix elements of the Hamiltonian are

$$H_{aa} = E_a, \quad H_{bb} = E_b, \quad H_{cc} = E_c,$$
$$H_{ab} = H_{ba} = -2\mu_{ab}\varepsilon_{ab} \cdot \cos(\omega_{ab}t),$$
$$H_{bc} = H_{cb} = -2\mu_{bc}\varepsilon_{bc} \cdot \cos(\omega_{bc}t); \tag{11 a-e}$$

E_g, $g = a$, b, c are the energies of the unperturbed molecule, $2\varepsilon_{ab}$ and $2\varepsilon_{bc}$ are the amplitudes of signal and pump microwave ω_{ab} and ω_{bc} its angular frequencies. As a volume element is considered the z dependence is eliminated. With (1) nine coupled differential equations are obtained:

$$i\dot{\varrho}_{aa} = -x_{ab}(\varrho_{ba} - \varrho_{ab}) \cdot \cos(\omega_{ab}t),$$
$$i\dot{\varrho}_{bb} = -x_{ab}(\varrho_{ab} - \varrho_{ba}) \cdot \cos(\omega_{ab}t)$$
$$\qquad -x_{bc}(\varrho_{cb} - \varrho_{bc}) \cdot \cos(\omega_{bc}t + \varphi),$$
$$i\dot{\varrho}_{cc} = -x_{bc}(\varrho_{bc} - \varrho_{cb}) \cdot \cos(\omega_{bc}t + \varphi),$$

$$i\dot{\varrho}_{ab} = \omega_0^{ab}\varrho_{ab} - x_{ab}(\varrho_{bb} - \varrho_{aa}) \cdot \cos(\omega_{ab}t)$$
$$+ x_{bc}\varrho_{ac} \cdot \cos(\omega_{bc}t + \varphi),$$

$$i\dot{\varrho}_{ba} = \omega_0^{ab}\varrho_{ba} - x_{ab}(\varrho_{aa} - \varrho_{bb}) \cdot \cos(\omega_{ab}t)$$
$$- x_{bc}\varrho_{ca} \cdot \cos(\omega_{bc}t + \varphi),$$

$$i\dot{\varrho}_{bc} = -\omega_0^{bc}\varrho_{bc} - x_{bc}(\varrho_{cc} - \varrho_{bb})$$
$$\cdot \cos(\omega_{bc}t + \varphi) - x_{ab}\varrho_{ac} \cdot \cos(\omega_{ab}t),$$

$$i\dot{\varrho}_{cb} = \omega_0^{bc}\varrho_{cb} - x_{bc}(\varrho_{bb} - \varrho_{cc}) \cdot \cos(\omega_{bc}t + \varphi)$$
$$+ x_{ab}\varrho_{ca} \cdot \cos(\omega_{ab}t),$$

$$i\dot{\varrho}_{ac} = -\omega_0^{ac}\varrho_{ac} - x_{ab}\varrho_{bc} \cdot \cos(\omega_{ab}t)$$
$$+ x_{bc}\varrho_{ab} \cdot \cos(\omega_{bc}t + \varphi),$$

$$i\dot{\varrho}_{ca} = \omega_0^{ac}\varrho_{ca} + x_{ab}\varrho_{cb} \cdot \cos(\omega_{ab}t)$$
$$- x_{bc}\varrho_{ba} \cdot \cos(\omega_{bc}t + \varphi),$$

$$x_{ij} = (2\mu_{ij}/\hbar)\,\varepsilon_{ij}, \quad \omega_0^{ij} = (E_i - E_j)/\hbar,$$
$$i, j = a, b, c. \tag{12 a–f}$$

Transforming to a rotating frame

$$\varrho_{aa} = \tilde{\varrho}_{aa}, \quad \varrho_{bb} = \tilde{\varrho}_{bb}, \quad \varrho_{cc} = \tilde{\varrho}_{cc},$$
$$\varrho_{ab} = \tilde{\varrho}_{ab} \cdot \exp(i\omega_{ab}t),$$
$$\varrho_{ba} = \tilde{\varrho}_{ba} \cdot \exp(-i\omega_{ab}t),$$
$$\varrho_{bc} = \tilde{\varrho}_{bc} \cdot \exp(i\omega_{bc}t),$$
$$\varrho_{cb} = \tilde{\varrho}_{cb} \cdot \exp(-i\omega_{bc}t),$$
$$\varrho_{ac} = \tilde{\varrho}_{ac} \cdot \exp(i\omega_{ac}t),$$
$$\varrho_{ca} = \tilde{\varrho}_{ca} \cdot \exp(-i\omega_{ac}t), \tag{13 a–i}$$

and using the rotating wave approximation and a second transformation:

$$s = \sum_g \tilde{\varrho}_{gg},$$
$$u_{gg'} = \tilde{\varrho}_{gg'} + \tilde{\varrho}_{g'g},$$
$$v_{gg'} = i(\tilde{\varrho}_{gg'} - \tilde{\varrho}_{g'g}),$$
$$w_{gg'} = \tilde{\varrho}_{gg} - \tilde{\varrho}_{g'g'},$$
$$g, g' = a, b, c \tag{14 a–d}$$

one gets after some calculations:

$$\dot{s} = 0,$$
$$\dot{u}_{ab} = -(\Delta\omega_{ab})v_{ab} + (x_{bc}/2)(v_{ac} \cdot \cos\varphi - u_{ac} \cdot \sin\varphi),$$
$$\dot{v}_{ab} = (\Delta\omega_{ab})u_{ab} - x_{ab}w_{ab}$$
$$- (x_{bc}/2)(u_{ac} \cdot \cos\varphi + v_{ac} \cdot \sin\varphi),$$
$$\dot{w}_{ab} = x_{ab}v_{ab} - (x_{bc}/2)(v_{bc} \cdot \cos\varphi - u_{bc} \cdot \sin\varphi),$$

$$\dot{u}_{bc} = -(\Delta\omega_{bc})v_{bc} + x_{bc}w_{bc} \cdot \sin\varphi - (x_{ab}/2)v_{ac},$$
$$\dot{v}_{bc} = (\Delta\omega_{bc})u_{bc} - x_{bc}w_{bc} \cdot \cos\varphi + (x_{ab}/2)u_{ac},$$
$$\dot{w}_{bc} = -(x_{ab}/2)v_{ab} + x_{bc}(v_{bc} \cdot \cos\varphi - u_{bc} \cdot \sin\varphi),$$
$$\dot{u}_{ac} = -(\Delta\omega_{ac})v_{ac} - (x_{ab}/2)v_{bc}$$
$$+ (x_{bc}/2)(u_{ab} \cdot \sin\varphi + v_{ab} \cdot \cos\varphi),$$
$$\dot{v}_{ac} = (\Delta\omega_{ac})u_{ac} + (x_{ab}/2)u_{bc}$$
$$- (x_{bc}/2)(u_{ab} \cdot \cos\varphi - v_{ab} \cdot \sin\varphi), \tag{15 a–i}$$

with

$$\Delta\omega_{gg'} = (E_{g'} - E_g)/\hbar - \omega_{gg'}.$$

Two special cases with $\varphi = 0$ and $\varphi = \pi$ are worked out for resonant signal, $\Delta\omega_{ab} = 0$, and resonant pump, $\Delta\omega_{bc} = 0$, microwaves. For the case when only pump radiation is present, $\varepsilon_{bc} \neq 0$, $\varepsilon_{ab} = 0$, one gets:

case $\varphi = 0$

$$\dot{s} = 0, \qquad\qquad \dot{u}_{bc} = 0,$$
$$\dot{u}_{ab} = (x_{bc}/2)v_{ac}, \quad \dot{v}_{bc} = -x_{bc}w_{bc},$$
$$\dot{v}_{ab} = -(x_{bc}/2)u_{ac}, \quad \dot{w}_{bc} = x_{bc}v_{bc},$$
$$\dot{w}_{ab} = -(x_{bc}/2)v_{bc}, \quad \dot{u}_{ac} = (x_{bc}/2)v_{ab},$$
$$\dot{v}_{ac} = -(x_{bc}/2)u_{ab}, \tag{16 a–i}$$

case $\varphi = \pi$

$$\dot{s} = 0, \qquad\qquad \dot{u}_{bc} = 0,$$
$$\dot{u}_{ab} = -(x_{bc}/2)v_{ac}, \quad \dot{v}_{bc} = x_{bc}w_{bc},$$
$$\dot{v}_{ab} = (x_{bc}/2)u_{ac}, \quad \dot{w}_{bc} = -x_{bc}v_{bc},$$
$$\dot{w}_{ab} = (x_{bc}/2)v_{bc}, \quad \dot{u}_{ac} = -(x_{bc}/2)v_{ab},$$
$$\dot{v}_{ac} = (x_{bc}/2)u_{ab}. \tag{17 a–i}$$

Next the solutions for the pulse sequence indicated in Fig. 6 are derived. This pulse sequence differs from the conditions used for the experiments illustrated in Fig. 5b and 5c. A simultaneous presence of signal and pump radiation would lead to more complicated solutions. The general features are not effected by the simplification of Figure 6.

For the time interval $t_1 - t_0$ of the resonant signal MW-pulse, $\varepsilon_{ab} \neq 0$, but $\varepsilon_{bc} = 0$, with the initial conditions:

$$u_{gg'}(t_0) = 0, \quad v_{gg'}(t_0) = 0, \quad w_{gg'}(t_0) \neq 0, \quad s(t_0) \neq 0,$$
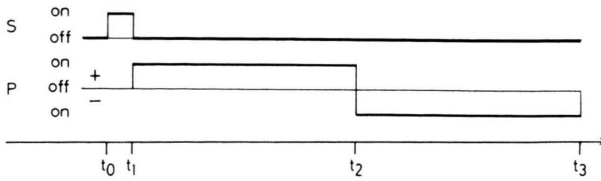$$g, g' = a, b \tag{18 a–d}$$

Fig. 6. Simplified pulse sequence used for the equations (19) to (21).

one gets solutions of the differential equations (15) partially of the form (7)

$$s(t_1 - t_0) \quad = s(t_0), \quad u_{ab}(t_1 - t_0) = 0,$$
$$v_{ab}(t_1 - t_0) = -w_{ab}(t_0) \cdot \sin[\varkappa_{ab}\varepsilon_{ab}(t_1 - t_0)],$$
$$w_{ab}(t_1 - t_0) = w_{ab}(t_0) \cdot \cos[\varkappa_{ab}\varepsilon_{ab}(t_1 - t_0)],$$
$$u_{bc}(t_1 - t_0) = 0, \quad v_{bc}(t_1 - t_0) = 0,$$
$$w_{bc}(t_1 - t_0) = w_{bc}(t_0) - (w_{ab}(t_0)/2)$$
$$\cdot \{1 - \cos[\varkappa_{ab}\varepsilon_{ab}(t_1 - t_0)]\},$$
$$u_{ac}(t_1 - t_0) = 0, \quad v_{ac}(t_1 - t_0) = 0. \quad (19\,a-i)$$

A polarization $v_{ab}(t_1 - t_0)$ is created, the occupation differences are changed.

The solutions (19) provide the initial conditions for the period $t_2 - t_1$, of the pump pulse with $\varphi = 0$, $\varepsilon_{bc} \neq 0$, but $\varepsilon_{ab} = 0$. The solutions of (16) for this period are:

$$s(t_2 - t_1) \quad = s(t_1 - t_0),$$
$$u_{ab}(t_2 - t_1) = 0,$$
$$v_{ab}(t_2 - t_1) = v_{ab}(t_1 - t_0) \cdot \cos[\varkappa_{bc}\varepsilon_{bc}(t_2 - t_1)/2],$$
$$w_{ab}(t_2 - t_1) = w_{ab}(t_1 - t_0) + w_{bc}(t_1 - t_0)$$
$$\cdot \{1 - \cos[\varkappa_{bc}\varepsilon_{bc}(t_2 - t_1)]\}/2,$$
$$u_{bc}(t_2 - t_1) = 0,$$
$$v_{bc}(t_2 - t_1) = -w_{bc}(t_1 - t_0) \cdot \sin[\varkappa_{bc}\varepsilon_{bc}(t_2 - t_1)],$$
$$w_{bc}(t_2 - t_1) = w_{bc}(t_1 - t_0) \cdot \cos[\varkappa_{bc}\varepsilon_{bc}(t_2 - t_1)],$$
$$u_{ac}(t_2 - t_1) = v_{ab}(t_1 - t_0) \cdot \sin[\varkappa_{bc}\varepsilon_{bc}(t_2 - t_1)/2],$$
$$v_{ac}(t_2 - t_1) = 0. \quad (20\,a-i)$$

By an appropriate length $t_2 - t_1 = \pi/(\varkappa_{bc}\varepsilon_{bc})$ the quantity $v_{ab}(t_2 - t_1)$, which is observed in the experiment, vanishes, while $u_{ac}(t_2 - t_1)$ reaches its maximum $v_{ab}(t_2 - t_1)$.

Under a continuous pump radiation the polarization $v_{ab}(t_2 - t_1)$ would oscillate with a Rabi frequency $\varkappa_{bc} \cdot \varepsilon_{bc}/2$ infinitely when relaxation is neglected.

In the following period $t_3 - t_2$ the phase φ of the pump microwave is inverted with the similar effect as discussed in the two level case. The Eqs. (17) have to be solved now with (20) as initial conditions

$$s(t_3 - t_2) \quad = s(t_1 - t_0),$$
$$u_{ab}(t_3 - t_2) = 0,$$
$$v_{ab}(t_3 - t_2) = v_{ab}(t_1 - t_0)$$
$$\cdot \cos\{\varkappa_{bc}\varepsilon_{bc}[(t_2 - t_1) - (t_3 - t_2)]/2\},$$
$$w_{ab}(t_3 - t_2) = w_{ab}(t_1 - t_0) + w_{bc}(t_1 - t_0)$$
$$\cdot \{1 - \cos[\varkappa_{bc}\varepsilon_{bc}((t_2 - t_1) - (t_3 - t_2))]\}/2,$$
$$u_{bc}(t_3 - t_2) = 0,$$
$$v_{bc}(t_3 - t_2) = -w_{bc}(t_1 - t_0)$$
$$\cdot \sin\{\varkappa_{bc}\varepsilon_{bc}[(t_2 - t_1) - (t_3 - t_2)]\},$$
$$w_{bc}(t_3 - t_2) = w_{bc}(t_1 - t_0)$$
$$\cdot \cos\{\varkappa_{bc}\varepsilon_{bc}[(t_2 - t_1) - (t_3 - t_2)]\},$$
$$u_{ac}(t_3 - t_2) = v_{ab}(t_1 - t_0)$$
$$\cdot \sin\{\varkappa_{bc}\varepsilon_{bc}[(t_2 - t_1) - (t_3 - t_2)]/2\},$$
$$v_{ac}(t_3 - t_2) = 0. \quad (21\,a-i)$$

By making both pump pulses of equal length the solutions (19) at time $t_1 - t_0$ are recovered. The phase inversion works as switching time in the reverse direction.

Influence of Mode Inhomogeneity on the Double Resonance Experiment

The mode inhomogeneity of the signal and pump radiation can be introduced into the solutions (19)–(21) by the same arguments as above. With $\varepsilon_{ab} = \varepsilon_{ab}^0 \sin(\pi x/a)$ and $\varepsilon_{bc} = \varepsilon_{bc}^0 \cdot \sin(n\pi x/a)$, $n = 1, 2 \ldots$ for H_{n0}-modes of the pump radiation for example $v_{ab}(t_2 - t_1)$ is modified to:

$$v_{ab}(t_2 - t_1) = -w_{ab}(t_0)$$
$$\cdot \sin\{\varkappa_{ab}\varepsilon_{ab}^0[\sin(\pi x/a)](t_1 - t_0)\}$$
$$\cdot \cos\{(\varkappa_{bc}/2)\varepsilon_{bc}^0[\sin(n\pi x/a)](t_2 - t_1)\}$$
$$= (-w_{ab}(t_0)/2)$$
$$\cdot \{\sin[\varkappa_{ab}\varepsilon_{ab}^0(\sin(\pi x/a))(t_1 - t_0)$$
$$+ (\varkappa_{bc}/2)\varepsilon_{bc}^0(\sin(n\pi x/a))(t_2 - t_1)]$$
$$+ \sin[\varkappa_{ab}\varepsilon_{ab}^0(\sin(\pi x/a))(t_1 - t_0)$$
$$- (\varkappa_{bc}/2)\varepsilon_{bc}^0(\sin(n\pi x/a))(t_2 - t_1)]\}.$$
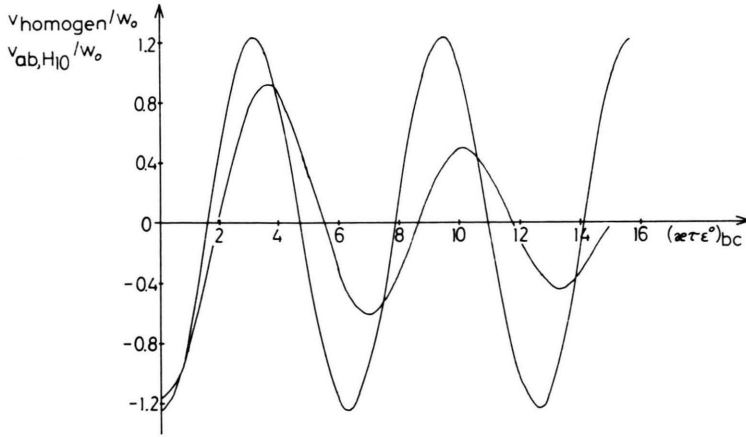$$(22)$$

Fig. 7. Comparison of solution (20b) $v_{\text{homogen}}/w_0(w_0 = w_{ab}(t_0))$, plane wave pump radiation assumed, with (24) $v_{abH_{10}}/w_0$ H_{10} pump mode assumed.
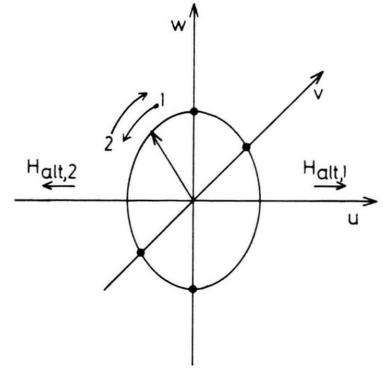
Fig. 8. NMR analog of a pulse experiment with a phase change of π described in a rotating system u, v, w. The carrier frequency of the pulse is resonant. $H_{\text{alt, 1}}$ magnetic field before phase change, $H_{\text{alt, 2}}$ magnetic field after phase change.

If one assumes the H_{10} mode of the pump radiation dominant one gets with $n = 1$:

$$
v_{ab}(t_2 - t_1) = (-w_{ab}(t_0)/2)
$$
$$
\cdot \{\sin[(\varkappa_{ab}\varepsilon_{ab}^0(t_1 - t_0)
$$
$$
+ (\varkappa_{bc}/2)\varepsilon_{bc}^0(t_2 - t_1)) \cdot \sin(\pi x/a)]
$$
$$
+ \sin[(\varkappa_{ab}\varepsilon_{ab}^0(t_1 - t_0)
$$
$$
- (\varkappa_{bc}/2)\varepsilon_{bc}^0(t_2 - t_1))
$$
$$
\cdot \sin(\pi x/a)]\} . \tag{23}
$$

Projecting $v_{ab}(t_2 - t_1)$ to the fundamental mode:

$$
v_{abH_{01}}(t_2 - t_1) = - w_{ab}(t_0) \{J_1[\varkappa_{ab}\varepsilon_{ab}^0(t_1 - t_0)
$$
$$
+ (\varkappa_{bc}/2)\varepsilon_{bc}^0(t_2 - t_1)]
$$
$$
+ J_1[\varkappa_{ab}\varepsilon_{ab}^0(t_1 - t_0)
$$
$$
- (\varkappa_{bc}/2)\varepsilon_{bc}^0(t_2 - t_1)]\} . \tag{24}
$$

In Fig. 7 we give a comparison to the case, where plane waves are assumed. Likewise into the other solutions of (20) and (21) the mode inhomogeneity may be introduced. The general behaviour with respect to time is thereby not changed. By two phase inverted pulses of equal length $t_3 - t_2 = t_2 - t_1$ the initial situation is reproduced. We think that the general features of the experiment are clarified. The relatively large line width of double resonance signals is mainly a consequence of the mode inhomogeneity of the pump radiation.

Appendix

In Fig. 8 we give for our first experiment the analogue in NMR. In a u, v, w space rotating about the w axis with angular velocity ω resonant to ω_0 the alternating magnetic field $H_{\text{alt, 1}}$ rotates coincident with u as a consequence of the rotating wave approximation. The Bloch vector of thermal equilibrium $(0, 0, w(t_0))$ precides clockwise with the Rabi frequency $\varkappa\varepsilon$ about the u-axis and stays for all times in the w, v-plane. If the phase of the radiation is changed by π the magnetic field switches to the u-direction ($H_{\text{alt, 2}}$). As a consequence the Bloch vector precides back. If both phase inverted pulses are of equal length the initial situation is recovered.

[1] H. Dreizler, E. Fliege, H. Mäder, and W. Stahl, Z. Naturforsch. **37a**, 1266 (1982).
[2] G. Bestmann, H. Dreizler, H. Mäder, and U. Andresen, Z. Naturforsch. **35a**, 392 (1980).
[3] G. Bestmann and H. Dreizler, Z. Naturforsch. **37a**, 58 (1982).
[4] G. Bestmann, H. Dreizler, E. Fliege, and W. Stahl, J. Mol. Struct. **97**, 215 (1983).
[5] W. Stahl, E. Fliege, H. Dreizler, and R. Schwarz, Z. Naturforsch. **39a**, 354 (1984).
[6] W. Stahl, G. Bestmann, H. Dreizler, U. Andresen, and R. Schwarz, Rev. Sci. Instrum. **56**, 1759 (1985).
[7] J. C. McGurk, T. G. Schmalz, and W. H. Flygare, Adv. in Chemical Physics **25**, 1 (1974), equation (159).
[8] H. Bomsdorf, H. Dreizler, and H. Mäder, Z. Naturforsch. **35a**, 723 (1980).
[9] l.c. [7] and Equation (113).
[10] l.c. [7], Chapter II.
[11] H. Mäder, J. Ekkers, W. Hoke, and W. H. Flygare, J. Chem. Phys. **62**, 4380 (1975).
[12] H. Mäder, J. Quant. Spectrosc. Radiat. Transf. **32**, 129 (1984).